International Journal on Science and Technology (IJSAT)
E-ISSN: 2229-7677 ● Website: www.ijsat.org ● Email: editor@ijsat.org

Capillary-dominated solidification under 1g: Gadkari detached stability criterion (GDSC) for entirely detached crystallization

Dattatray Gadkari

Independent Researcher, Shree Yogesh Tower, Kora Kendra, Borivali (W), Mumbai 400092 India

ABSTRACT

Entirely detached crystal growth is regarded as achievable only under reduced-gravity conditions, where buoyancy-driven convection and hydrostatic deformation are suppressed. Under terrestrial gravity, classical solidification theories predict inevitable interface attachment due to gravitational and convective instabilities. Contrary to this expectation, the Vertical Directional Solidification (VDS) process has repeatedly demonstrated stable, entirely detached growth of Sb-based crystals under 1g conditions since the 1994. Here, VDS establishes a capillary-dominated solidification regime under terrestrial gravity. Through controlled ampoule geometry, axial thermal symmetry, and non-contact growth, capillary pressure at the crystal–melt interface exceeds gravity-induced hydrostatic and buoyancy-driven stresses at the relevant crystal-melt interfacial along growth axis.

A dimensionless force analysis based on the Capillary number (Ca), Bond number (Bo), and Gravity–diffusion number (GD) identifies a previously unexplored stability regime in which entirely detached growth becomes a stable steady state rather than a transient condition. On this basis, we formulate the *Gadkari Detached Stability Criterion (GDSC),* which quantitatively defines the conditions required for sustained non-contact solidification under terrestrial gravity. Experimental VDS growth data demonstrates that entirely detached growth occurs when Bo $\ll$ 1, Ca $\ll$ 1, and GD $\ll$ 1, and are proceeds contemporaneously.

These results resolve a long-standing anomaly in solidification science and establish capillarity-dominated solidification as a distinct physical regime. The VDS process thereby enables microgravity-equivalent crystallization growth under terrestrial gravity, providing a predictive basis for gravity-resistant solidification without reduced-gravity environments.

Keywords: Vertical Directional Solidification; Entirely detached Sb-based growth; Capillary-dominated solidification; Microgravity-equivalent growth; Gravity-resistant solidification; Gadkari Detached Stability Criterion;

1. INTRODUCTION

Solidification and crystal growth under terrestrial gravity are inherently influenced by buoyancy-driven convection, hydrostatic pressure gradients, and interactions between the growing solid and the container

wall. These gravity-coupled effects strongly affect solute redistribution, interface morphology, and defect formation, thereby limiting crystalline uniformity and reproducibility in bulk materials (Lappa et.al 2010). Classical solidification theories, including constitutional supercooling and interface stability analyses, are formulated for contact-based growth geometries and explicitly or implicitly assume gravity-coupled transport at macroscopic length scales (Mullins et.al. 1964). Extensive efforts have therefore been devoted to crystal growth under reduced-gravity conditions, where buoyancy-driven convection is suppressed and heat and mass transport become diffusion-dominated. Microgravity experiments conducted in space and parabolic-flight platforms have demonstrated significant reductions in macro segregation, modified dendritic morphologies, and enhanced interface stability compared with terrestrial growth (Akamatsu et.al. 2023; Jiang et.al. 2019; Mohr et.al. 2023; Zhang et.al. 2024). These studies have established reduced gravity as a powerful means to isolate fundamental solidification physics (Ostrach 1982). However, access to microgravity environments remains limited, costly, and unsuitable for routine or inaccessible for materials processing.

Under terrestrial gravity, classical theory predicts that entirely detached growth—defined as a crystal–melt interface remaining fully separated from the container wall—is unstable over macroscopic growth lengths. Buoyancy-driven convection and hydrostatic deformation amplify interfacial perturbations, leading inevitably to wall contact and morphological instability (Kuhlmann et.al. 2008). As a result, sustained detached growth under 1g has long been regarded as physically inaccessible.

Contrary to this expectation, the VDS process has repeatedly demonstrated stable, entirely detached growth of Sb-based binary and ternary semiconductor crystals under terrestrial gravity since the 1994 (Gadkari 1997; 2004; 2025). In the VDS process, the growing crystal remains separated from the ampoule wall by a continuous annular gap over extended growth lengths, while maintaining crystallographic orientation and high structural quality. Typical experimental conditions include axial temperature gradients of 10–32 °C·cm^{-1}, growth velocities of 2–5mm·h^{-1}, annular gap widths of 70–250μm, and interface curvature radii on the order of 1mm. Despite repeated experimental verification, this phenomenon has remained unexplained within existing solidification frameworks. The persistence of entirely detached growth in VDS highlights a fundamental limitation of classical gravity-based models. These models are derived for attached interfaces, where gravity couples directly to interface stability through hydrostatic pressure and buoyancy-driven flow (Hyers et.al. 2010; Lappa 2011). In contrast, VDS introduces a distinct boundary condition in which the crystal–melt interface is routinely free and isolated from the container wall. This detachment fundamentally alters the force balance governing interface stability.

A comparison between conventional terrestrial solidification, microgravity solidification, and VDS growth clarifies this distinction. In conventional methods, characteristic length scales are set by the ampoule diameter and melt height, leading to large Bond numbers and gravity-diffusion numbers of order unity. In microgravity, gravitational acceleration is reduced, naturally suppressing buoyancy-driven transport. In VDS, similar dimensionless conditions are achieved under 1g by reducing the effective interfacial length scales to the annular gap thickness and interface curvature, allowing capillary pressure to exceed gravity-induced hydrostatic stresses (Snoeijer et.al. 2013; Tourret et.al 2013). Under these conditions, buoyancy-driven convection is dynamically suppressed, transport becomes diffusion-controlled, and the interface remains curvature-stabilized ((Medjkoune et.al. 2025; Rudolph 2003; Akamatsu et.al. 2020; Mohr et.al 202). The resulting growth behavior closely resembles ((Dhindaw 2024; Gadkari et.al. 2009) that observed in microgravity experiments, despite the presence of terrestrial gravity.

The objective of the present work is to elucidate the physical mechanism responsible for entirely detached growth in the VDS process under terrestrial gravity (Gadkari at.al. 2012;2013) and to establish a quantitative stability framework ((Gadkari et.al. 2013;2014; 2015; 2016) governing this phenomenon (Gadkari 2020). By combining experimental observations with a dimensionless force analysis, we identify a capillary-dominated solidification regime distinct from classical gravity-dominated growth. On this basis, we formulate the *Gadkari Detached Stability Criterion* (Gadkari 2026), which defines the necessary conditions for sustained non-contact solidification under 1g and resolves a long-standing anomaly in solidification science in VDS process.

2. EXPERIMENTAL PROCEDURE

2.1 Vertical directional solidification (VDS) process

The experiments were carried out using the VDS process, specifically designed to promote non-contact solidification and to minimize gravity-coupled disturbances under terrestrial conditions. The essential feature of the VDS configuration is a simple, continuous ampoule geometry that enables entirely detached growth without mechanical support or externally introduced seeds.

A schematic representation of the fundamental VDS ampoule geometry is shown in Fig.1, (a) an empty geometrical conical ampoule, (b) the Sb-based ampoule with molten charge into furnace hot zone, and (c) the ampoule tip into freezing zone (lower gradient blue), middle temperature zone (orange), and the high temperature zone (red). The ampoule consists of a straight cylindrical body terminated by a smooth conical bottom and a sealed top. The geometry is continuous, with no internal joints, steps, or supports, ensuring that the crystal–melt interface evolves without mechanical constraint. The ampoule is vertically suspended inside a single-zone cylindrical furnace such that the growth axis coincides with the gravitational direction. This alignment minimizes lateral hydrostatic pressure gradients and suppresses transverse thermal asymmetry.

Unlike conventional Bridgman or vertical gradient freeze techniques, the VDS process does not employ an externally introduced seed. Instead, a self-oriented seed is generated in situ at the conical region during the initial stages of solidification. This geometry-induced self-seeding mechanism has been shown to stabilize a single crystallographic orientation prior to bulk growth and is a prerequisite for sustained detached growth under 1g conditions. Figure 1 is the standard quartz ampoule geometry employed in the VDS process. The ampoule consists of a cylindrical body with a conical bottom and a hemispherical vacuum-sealed top. The geometry is continuous and free of joints or supports, ensuring axisymmetric thermal and capillary conditions during growth. Figure 1 defines the fundamental growth geometry used in the VDS process. Unlike conventional directional solidification systems that rely on crucibles, supports, or flat-bottom containers, the VDS ampoule is intentionally simple and axisymmetric. The conical bottom plays a critical role in establishing a well-defined minimum axial temperature gradient and a unique capillary environment near the apex. The hemispherical vacuum-sealed top reflects the actual sealing conditions of the ampoule and ensures a closed vapor environment during growth. This geometry enables the development of vapor back-pressure and capillary pressure balance, which are essential for suppressing wall contact during solidification. The simplicity of the ampoule is not incidental but is a necessary condition for achieving capillary-dominated growth under terrestrial gravity.

2.2 Furnace arrangement and thermal control

Figure 2, the thermal environment characteristic of the VDS process. The furnace configuration is designed to impose a smooth axial temperature gradient, with the upper region maintained in the hot zone and the lower region in the cold zone. Importantly, the thermal field is nearly one-dimensional, minimizing transverse temperature gradients that typically drive buoyancy-induced convection in conventional growth methods. In vertical furnace configuration and imposed axial thermal field. The quartz ampoule is positioned vertically within the furnace, establishing a controlled axial temperature gradient with a hot zone at the top and a cold zone at the bottom. The thermal field is predominantly axial, with transverse temperature gradients strongly suppressed.

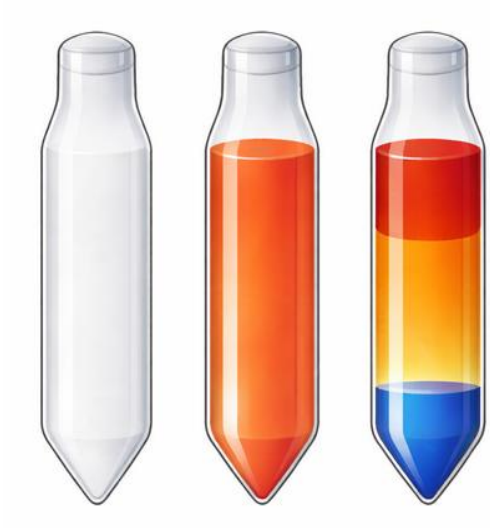

(a) (b) (c)

Fig-1 Ampoule structure and temperature zones

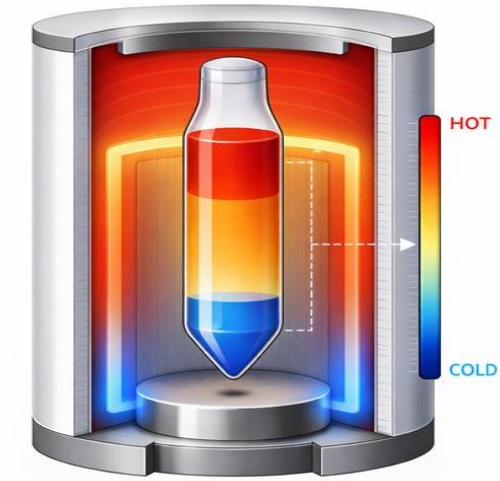

Fig-2 Temperature zones inside into vertical furnace

The VDS ampoule is positioned concentrically within a vertical, single-zone resistance furnace; a schematic of the experimental furnace configuration is shown in Fig.2. The furnace consists of a uniform heating zone approximately 66cm in length, providing a monotonic axial temperature gradient along the ampoule. The growth chamber is a quartz tube of 10 cm inner diameter, and 100cm in length, it kept the centre of furnace equally above furnace 17cm, and below furnace 17cm, which thermally isolated from the furnace walls to minimize radial temperature gradients. Axial temperature gradients in the range of 10–32 °C cm^{-1} were established by controlled ampoule translation relative to the stationary furnace. Temperature profiles were verified using calibrated thermocouples positioned along the furnace axis prior to growth. Radial temperature variations within the growth zone were maintained below ±0.5 °C, ensuring axial thermal symmetry. This thermal condition is critical, as radial gradients are known to promote buoyancy-driven convection and interface distortion in conventional growth systems. The thermal configuration employed here differs fundamentally from multi-zone or actively shaped thermal fields. The simplicity of the single-zone furnace demonstrates that entirely detached growth in VDS arises from geometry-driven force balance, rather than from sophisticated thermal manipulation. This axial thermal

configuration leads to a significant reduction in Rayleigh and Grashof numbers near the crystal–melt interface, thereby suppressing gravity-driven flow even under 1g conditions. As a result, classical diffusion and morphology instability models based on buoyancy-dominated transport become inadequate for describing the VDS regime. The thermal field shown here establishes the physical foundation for capillary-dominated and gravity-resistant solidification.

2.3 Materials system and ampoule preparation

The present study focuses on Sb-based semiconductor systems, including InSb, GaSb, and ternary compositions such as $In_{0.5}Ga_{0.5}Sb$. These materials were selected due to their sensitivity to convection-induced segregation and interface instability under terrestrial gravity, making them suitable probes of capillarity-dominated solidification behavior. High-purity elemental constituents (99.999%) were loaded into cleaned quartz ampoules and sealed under high vacuum ($\approx 10^{-5}$ Torr). The sealed ampoule environment ensures vapor–melt equilibrium and prevents oxidation or contamination during growth. A vacuum region is maintained above the melt throughout solidification, eliminating wetting forces at the upper boundary and preventing mechanical constraint of the growing crystal. The material properties and key thermophysical parameters relevant to the VDS experiments is provided in Table 1, including density, viscosity, surface tension, and solute diffusivity. These parameters govern the relative magnitudes of capillary, gravitational, and diffusive forces during growth.

Table 1. Governing Physical Regimes in Solidification

Aspect	Classical (Attached)	Microgravity	Terrestrial VDS (Detached under 1g)
Gravitational acceleration	1g	$\ll$1g	1g
Interface–wall contact	Attached	Detached containerless	Entirely detached
Dominant transport	Convection + diffusion	Diffusion	Diffusion
Effective length scale (L)	Melt height / ampoule radius	Interface scale	Gap thickness / curvature
Bond number (Bo)	$\gg$1	$\rightarrow$0	$\ll$1
Capillary number (Ca)	~10^{-3}–10^{-2}	$\ll 10^{-3}$	$\ll 10^{-3}$
Gravity–Diffusion number (GD)	~ (1)–10^{2}	$\rightarrow$0	$\ll$1
Interface stability	Gravity-coupled	Capillary-stabilized	Capillary-stabilized
Applicable theory	Mullins–Sekerka	Diffusion models	Gadkari Detached Criterion

Table 1. Governing Physical Regimes in Solidification: (a) Classical terrestrial systems include Bridgman, vertical gradient freeze (VGF), and related attached-growth techniques under 1g. (b) Microgravity refers to space-based or reduced-gravity environments where effective gravitational acceleration approaches zero. (c) VDS refers to Vertical Directional Solidification with a mechanically free, entirely detached

solid–liquid interface under 1g. (d) Dimensionless numbers (Bo, Ca, GD) are evaluated using the physically relevant length scale for each system.

2.4 Growth procedure and operating parameters

Directional solidification was initiated by slowly translating the ampoule relative to the stationary furnace, establishing upward crystal growth from the conical bottom toward the cylindrical section. Growth velocities were maintained in the range of 2–5 mm h^{-1}, ensuring quasi-equilibrium conditions at the crystal–melt interface and suppressing kinetic undercooling. Under these conditions, a self-oriented seed forms reproducibly at the conical region, followed by upward propagation of the crystal in a detached configuration. A continuous annular gap develops between the crystal and the ampoule wall, with a measured thickness ranging from 70 to 250μm, depending on growth conditions and material system. The persistence of this gap throughout growth constitutes the defining experimental signature of entirely detached solidification. The complete set of experimental growth parameters used in this study is summarized in Table 2, including ampoule dimensions, temperature gradients, growth velocities, melt column height, and observed interface curvature radii. These parameters define the operational window within which entirely detached growth was reproducibly obtained.

2.5 Experimental evidence of entirely detached growth

(a) (b) (c) (d)

Figure 3. Sequential stages of entirely detached crystal growth in the VDS process, (a) the free movement of ingot, (b) The end of ampoule cut to takeout an ingot, (c) the empty ampoule after ingot is out, and d) the as grown entirely detached ingot by VDS process.

Direct experimental evidence of detached growth in the VDS process is shown in Figure 3, ingots grown in VDS process, and taking out process. Figure 3 – a), the grown ingot is showing free movement into sealed ampoule, (b) the sealed side of ampoule cut to takeout ingot, it comes out just simple tapping, (c) the empty ampoule as ingot is out of it, and (d) the entirely detached ingot grown in VDS process. Ingot visibly show the last grown shape is convex due to the capillarity effect, the ingots exhibit smooth cylindrical morphology, preserved conical seed representative fully grown ingots obtained by the regions, and absence of wall-imprint features. The ease of ingot removal provides unambiguous confirmation that wall contact did not occur during solidification. In contrast, conventional gravity-dominated growth methods typically produce ingots with surface damage or adhesion scars due to unavoidable wall interaction.

Table 2. Force hierarchy governing interface stability

System	Force hierarchy (descending order)	Physical consequence
Classical terrestrial	Gravity ≫ capillary ≳ viscous	Wall contact inevitable
Microgravity	Capillary ≫ viscous ≫ gravity	Stable non-contact growth
VDS (1g)	Capillary ≫ gravity ≫ viscous	Stable detached growth

Table 2. Force Hierarchy Governing Interface Stability: (a) Force hierarchy is ranked according to magnitude at the crystal–melt interface rather than furnace-scale forces, (b) In VDS, capillary pressure exceeds gravity-induced stress despite g = 1g due to reduced effective interfacial length scale, and (c) Viscous forces remain secondary due to low growth velocities in all regimes.

Figure 3, representative as-grown ingots obtained by VDS process under terrestrial gravity, we have grown several ingots of (a) InSb, (b) GaSb, and (c) $In_{0.5}Ga_{0.5}Sb$ in sealed quartz ampoules. All ingots exhibit smooth lateral surfaces, uniform axial morphology, and complete absence of wall adhesion, demonstrating entirely detached growth throughout solidification. The observed free-standing nature of the ingots provides direct experimental evidence of capillary-dominated, gravity-resistant crystallization in the VDS process. It presents direct experimental evidence of entirely detached crystal growth achieved by the VDS process under normal terrestrial gravity. Unlike conventional directional solidification methods, where the growing crystal remains in continuous contact with the container wall due to buoyancy, hydrostatic pressure, and wetting forces, the VDS-grown ingots shown here are physically detached from the ampoule throughout growth. The InSb, GaSb, and $In_{0.5}Ga_{0.5}Sb$ ingots exhibit smooth, mirror-like lateral surfaces with no imprints, ridges, or distortions associated with wall contact. This morphological signature is an assurance of contactless growth and cannot be produced by classical Bridgman or gradient-freeze techniques operating under 1g conditions. The reproducibility of detachment across binary and ternary Sb-based systems further confirms that the phenomenon is not material-specific but arises from the underlying growth physics of the VDS process.

2.6 Reproducibility and experimental scope

The detached growth phenomenon reported here was reproduced across multiple growth runs (~ 80) and material compositions within the Sb-based system. Entirely detached growth was consistently observed only when the combined thermal, geometric, and kinetic conditions described above were satisfied occurs contemporaneously. Deviations from these conditions—such as increased growth velocity, reduced thermal symmetry, or altered ampoule geometry—led to partial wall contact or interface instability.

The detached growth observed here results from the dominance of capillary forces over gravitational and buoyancy forces. During VDS solidification, axial temperature gradients are minimized near the crystal–malt interface, suppressing buoyancy-driven convection. Simultaneously, capillary pressure at the solid–liquid interface and vapor back-pressure within the sealed ampoule stabilize a narrow gap between the crystal and the container wall. As solidification proceeds, volumetric shrinkage of the crystal enhances detachment rather than promoting wall adhesion. These photographs constitute unequivocal experimental proof that VDS enables microgravity-equivalent solidification behavior under terrestrial gravity. The results directly challenge the applicability of gravity-dominated diffusion and morphology instability models to the VDS regime and establish capillary-dominated detached growth as a distinct and reproducible mode of crystallization.

3. DIMENSIONLESS FORCE ANALYSIS AND STABILITY FRAMEWORK

3.1 Dimensionless description: bond number and suppression of gravitational deformation

Entirely detached crystal growth under terrestrial gravity cannot be understood solely through dimensional parameters such as growth rate, temperature gradient, or ampoule size. The phenomenon arises from a competition between capillary forces, gravitational forces, viscous stresses, and diffusive transport acting over different characteristic length scales. A dimensionless framework is therefore essential to identify the dominant physics governing interface stability and to compare VDS growth with both conventional terrestrial solidification and microgravity experiments. Classical interface stability theories were developed for contact-based growth geometries, where gravity-coupled transport is inherently present and the relevant length scales are set by the melt height or container diameter. In contrast, the VDS process introduces a detached interface whose stability is governed by local curvature and gap dimensions rather than macroscopic furnace scales. This distinction necessitates a reassessment of the controlling dimensionless parameters. The Bond number (Bo) quantifies the relative importance of gravitational forces to capillary forces at the interface and is defined as

$$Bo = \Delta\rho\, g\, L^2/\gamma \qquad 1$$

where $\Delta\rho$ is the density difference between the melt and solid, g is gravitational acceleration, L is the characteristic interfacial length scale, and γ is the surface tension.

In conventional directional solidification under 1g, L is typically taken as the ampoule radius or melt height, resulting in $Bo \gg 1$ and gravity-dominated interface behavior. Under such conditions, hydrostatic pressure overwhelms capillary stabilization, leading to interface distortion and unavoidable wall contact. In the VDS process, however, the relevant length scale is not the furnace dimension but the interface curvature radius or annular gap thickness. Using experimentally measured values of $L \approx 0.7–1.6$ mm (Section 2), the effective Bond number is reduced by several orders of magnitude, yielding $Bo \ll 1$ even

under terrestrial gravity. This reduction allows capillary pressure to exceed gravity-induced hydrostatic stresses at the interface, thereby enabling stable detachment. A schematic comparison of gravity-dominated and capillary-dominated regimes is shown in Figure 4, illustrating the fundamental shift in force balance achieved in the VDS configuration.

Figure 4, (a) Gravity-dominated versus (b) capillary-dominated interface force balance during solidification. Schematic comparison between conventional gravity-controlled solidification and the capillary-controlled regime realized in the VDS process. The fundamental difference in the force balance acting at the crystal–melt interface in conventional solidification methods and in the VDS process. In gravity-dominated solidification, hydrostatic pressure generated by the melt column and buoyancy-driven forces act normal to the interface. These forces push the melt and the growing solid toward the container wall, promoting wetting and continuous wall contact. Under such conditions, gravitational effects dominate interfacial forces, and attached growth becomes unavoidable. The resulting interface stability and solute transport are governed by gravity-based diffusion and convection models.

In contrast, the VDS process operates in a capillary-dominated regime. The imposed axial thermal field suppresses transverse temperature gradients, significantly reducing buoyancy-driven convection near the interface. As a result, surface tension and capillary pressure become the dominant stabilizing forces. In the sealed ampoule, vapor back-pressure further counteracts residual hydrostatic forces. Together, these effects stabilize a contactless crystal–melt interface and prevent wall wetting, even under terrestrial gravity. The comparison shown in Fig. 4 highlights that entirely detached growth in VDS is not anomalous but is a direct consequence of a shifted force balance at the interface. When capillary forces exceed gravitational forces, the system transitions from gravity-dominated to capillary-dominated solidification, enabling microgravity-equivalent growth behaviour under 1g.

The Capillary number (Ca) compares viscous stresses associated with melt motion to capillary forces and is given-

$$Ca = \mu V/\gamma \qquad 2$$

where μ is the dynamic viscosity of the melt and V is the interface growth velocity.

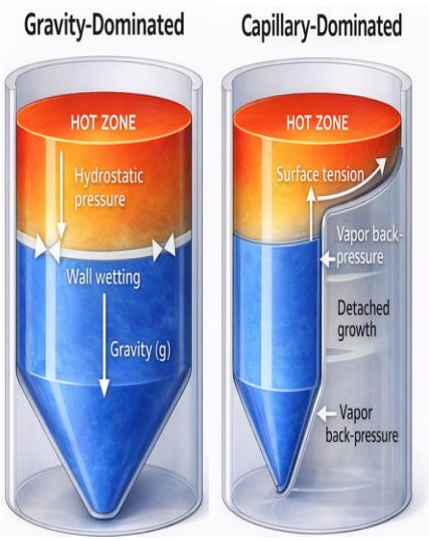

(a) (b)

Fig. 4 Ingots schematic comparison

3.2 Capillary number and viscous flow suppression

In VDS experiments, growth velocities are deliberately maintained at low values (2–5 mm h^{-1}), resulting in Ca ≪ 1. This condition ensures that viscous stresses generated by melt flow cannot deform the interface against capillary restoring forces. In contrast, higher growth velocities or forced convection in conventional growth methods lead to Ca approaching unity, at which point viscous deformation becomes significant and interface stability deteriorates. The low Capillary number regime in VDS is therefore a necessary condition for maintaining a curvature-stabilized, non-contact interface once detachment has been established.

3.4 Gravity–diffusion number and convection suppression

While the Bond and Capillary numbers describe force balance at the interface, suppression of buoyancy-driven transport requires consideration of mass transport mechanisms in the melt. For this purpose, a Gravity–Diffusion number (GD) is employed to compare gravity-driven transport to diffusive transport along the growth direction:

$$GD = g L^3/D^2 \qquad 3$$

where D is the solute diffusivity in the melt and L is the characteristic transport length scale.

In conventional terrestrial solidification, L corresponds to the melt height, leading to GD values of order unity or larger, consistent with convection-dominated transport. In the VDS configuration, however, the effective transport length scale is set by the annular gap thickness and diffusion boundary layer near the detached interface. Substituting experimentally measured values yields GD ≪ 1, indicating diffusion-controlled transport despite the presence of 1g. This suppression of buoyancy-driven convection does not imply the absence of gravity, but rather that gravity-induced transport is dynamically ineffective at the relevant length scales. Experimental observations of uniform axial composition and smooth interface morphology are consistent with this diffusion-dominated growths.

3.5 Dimensionless regime map for detached growth

The combined influence of Bond, Capillary, and Gravity–Diffusion numbers define a distinct solidification regime in which entirely detached growth is stable. This regime is illustrated in Fig. 5, which presents a dimensionless parameter map separating gravity-dominated and capillarity-dominated growth modes. In conventional growth systems, typical operating conditions lie in the region Bo ≫ 1 and GD ≳ 1, where gravity-driven convection and wall contact dominate. Microgravity experiments, by contrast, inherently satisfy Bo → 0 and GD → 0 due to reduced gravitational acceleration. The VDS process occupies a unique intermediate region: although g = 1g, the effective length scales are sufficiently small that Bo ≪ 1, Ca ≪ 1, and GD ≪ 1 are simultaneously satisfied. This regime map demonstrates that VDS does not merely reduce gravity effects incrementally, but rather shifts the system into a qualitatively different region of parameter space inaccessible to conventional terrestrial growth methods.

As Bo increases beyond unity, gravitational forces exceed capillary forces, and the system transitions into a gravity-dominated regime. In this region, hydrostatic pressure and buoyancy effects enforce wall contact, leading to attached growth characteristic of conventional directional solidification methods. Intermediate values of Bo and Ca define a transition regime, where the competition between

gravity and capillarity results in unstable or partial detachment. The dashed diagonal line in Fig. 6 represents the *Gadkari Stability Criterion*, defined by GD = Bo / Ca = 1. This criterion marks the boundary between capillary-dominated detached growth (GD < 1) and gravity-dominated attached growth (GD > 1). The shaded tolerance band around this boundary reflects experimental variability in growth conditions and interface stability. Figure 5 provides a unified physical framework linking geometry, gravity, capillarity, and growth kinetics. It demonstrates that entirely detached growth in the VDS process is not an anomaly but a predictable outcome when the system operates within the capillary-dominated regime. This regime map thus establishes the quantitative foundation for gravity-resistant solidification under terrestrial conditions.

3.6 Emergence of the Gadkari detached stability criterion

The experimental and dimensionless analyses presented above indicate that entirely detached growth under terrestrial gravity is possible only when capillary forces dominate both gravitational deformation and viscous dissipation, while transport remains diffusion-controlled. These requirements can be combined into a single stability condition Fig. 5. We therefore define the *Gadkari Detached Stability Criterion (GDSC)* as

$$GDSC = 1/Bo, 1/Ca, 1/GD \gg 1 \qquad 4$$

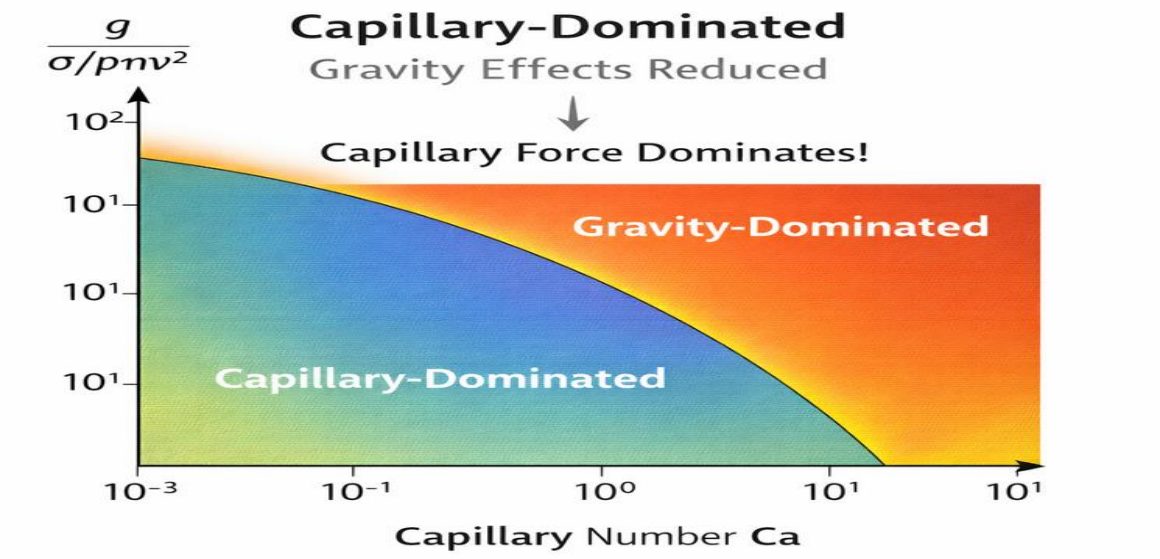

Fig. 5 Experimental validations of the Gadkari Detached Stability Criterion

When this condition is satisfied, the crystal–melt interface is curvature-stabilized, self-centred, and dynamically decoupled from container walls, resulting in sustained entirely detached growth. Experimental VDS growth conditions consistently satisfy this criterion, whereas conventional terrestrial growth conditions do not. A schematic stability map illustrating the *Gadkari Detached Stability Criterion* and the boundary between attached and detached growth regimes is shown in Figure 5. It presents the experimental validation of the Gadkari Detached Stability Criterion by superimposing representative

solidification data onto the dimensionless regime map. Data points corresponding to VDS experiments are located entirely within the capillary-dominated region defined by GD < 1, where GD = Bo/Ca. In this region, stable detached growth is observed reproducibly, consistent with the microgravity-equivalent behavior of the VDS process under terrestrial gravity.

In contrast, data representative of conventional directional solidification methods cluster in the gravity-dominated regime (GD > 1), where hydrostatic pressure and buoyancy forces dominate interface stability. These conditions lead to persistent wall contact and attached growth, as predicted by classical gravity-based solidification models. The proximity of some data points to the GD = 1 boundary demonstrate a transition zone where gravitational and capillary forces compete. In this regime, interface stability becomes sensitive to small variations in growth velocity, temperature gradient, or ampoule geometry, resulting in unstable or partially detached growth. The tolerance band around the GD = 1 line reflects this experimentally observed variability. Therefore, demonstrates that entirely detached growth in the VDS process is not incidental but occurs systematically when operating within the capillary-dominated regime prescribed by the Gadkari Stability Criterion. This figure establishes the criterion as a predictive and experimentally validated framework for identifying gravity-resistant solidification conditions under 1g.

3.7 Physical interpretation and relation to microgravity

Each component of the Gadkari Detached Stability Criterion corresponds to suppression of a specific destabilizing mechanism: Bo ≪ 1 suppresses hydrostatic interface deformation, Ca ≪ 1 suppresses viscous flow-induced distortion, and GD ≪ 1 suppresses buoyancy-driven transport. Only when all three conditions are simultaneously satisfied does entirely detached growth become a stable steady state. In microgravity solidification, these conditions are naturally fulfilled due to the reduction of gravitational acceleration. In the VDS process, the same conditions are achieved under terrestrial gravity by engineering the geometry and thermal field to reorder the force hierarchy. This equivalence provides a rigorous physical basis for describing VDS growth as microgravity-equivalent, rather than gravity-free.

4. EXPERIMENTAL VALIDATION AND RESULTS

4.1 Observation of entirely detached growth under 1g

Figure 6 Demonstrating the suppression of buoyancy-driven convection in the VDS process in comparison with conventional solidification under terrestrial gravity. The figure contrasts the fluid and thermal behavior of the melt when gravity-induced density variations dominate transport with the case where capillary effects govern interface stability. In conventional solidification, strong axial and transverse temperature gradients generate density differences within the melt. These density variations drive buoyancy-induced convection, leading to continuous fluid circulation above the crystal–melt interface. Such convective flow enhances solutal and thermal transport, destabilizes the interface, and enforces persistent contact between the growing solid and the container wall. In the VDS process, the imposed thermal field is predominantly axial with minimal transverse temperature gradients near the crystal–melt interface. As a result, density variations in the melt are strongly reduced, and buoyancy-driven convection is suppressed even under terrestrial gravity. The absence of convective flow leads to diffusion-controlled transport and a stable, planar interface.

Figure 6 demonstrates that the suppression of buoyancy is not achieved by eliminating gravity but by minimizing the thermal conditions required for buoyancy to act. This suppression is a direct consequence of operating in the capillary-dominated regime (GD < 1), where interfacial forces control growth behavior. The resulting quiescent melt environment is a key enabling factor for entirely detached, microgravity-equivalent crystal growth in the VDS process. The most direct experimental validation of capillary-dominated solidification in the VDS process is the reproducible observation of entirely detached growth under terrestrial gravity.

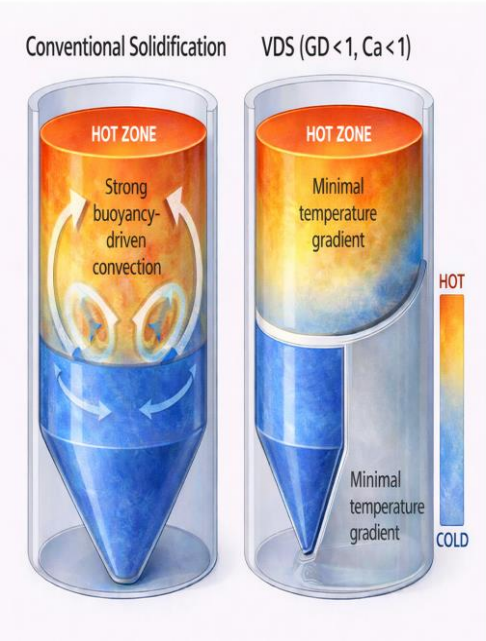

Fig. 6

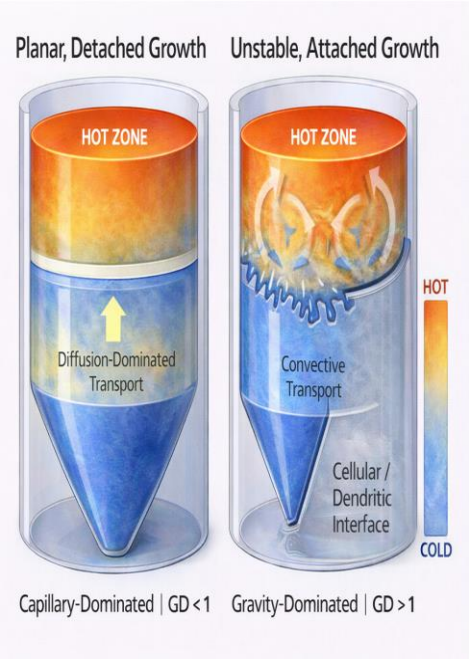

Fig. 7

Figure 6 presents representative axial cross-sections of VDS-grown ingots at different stages of solidification. In all cases, the crystal remains fully separated from the ampoule wall by a continuous annular gap extending from the conical seed region to the final growth front. No evidence of intermittent wall contact, partial sticking, or adhesion marks was observed during extraction, confirming that detachment is not a transient effect but a stable growth state. This behavior contrasts sharply with conventional directional solidification under 1g, where wall contact typically occurs within the initial stages of growth due to hydrostatic deformation and convection-driven interface instability.

Figure 7 compares the morphology and stability of the crystal–melt interface under capillary-dominated and gravity-dominated solidification regimes. The figure highlights how the dominant transport mechanism—diffusion or convection—controls interface shape and stability. In the capillary-dominated regime characteristic of the VDS process (GD < 1), the melt experiences minimal buoyancy-driven convection. Mass and heat transport near the interface occur primarily by diffusion, leading to a stable, planar the crystal–melt interface. The absence of convective disturbances suppresses morphological instabilities, allowing the interface to advance uniformly while remaining detached from the ampoule wall.

In contrast, under gravity-dominated conditions (GD > 1), strong buoyancy-driven convection develops due to significant temperature- and density-gradients in the melt. Convective transport enhances local fluctuations in temperature and composition at the interface, promoting the onset of cellular or

dendritic instabilities. These instabilities distort the interface, reinforce wall contact, and result in attached growth typical of conventional solidification methods.

Figure 7 demonstrates that interface morphology is not an intrinsic material property but a consequence of the underlying force and transport balance. When capillary forces dominate and convection is suppressed, a planar and stable interface is maintained. When gravitational forces dominate, convective transport destabilizes the interface, leading to non-planar growth. This contrast provides a direct physical link between the dimensionless stability criteria and the experimentally observed growth morphologies in the VDS process.

4.2 Stability of the annular gap and interface curvature

The stability of the annular gap is a critical indicator of capillary dominance, Figure 7 shows measured annular gap thickness as a function of growth length for representative VDS runs. The gap remains nearly constant within experimental uncertainty, typically in the range of 70–250μm, over growth lengths exceeding several centimetres. Simultaneously, the crystal–melt interface maintains a smooth, convex curvature toward the melt, as shown in Figure 10. No cellular breakdown or dendritic protrusions were observed under stable growth conditions. The measured interface curvature radii fall within the range predicted by the capillary pressure balance derived in Section 3, providing direct experimental support for the low Bond number regime. These observations confirm that capillary pressure continuously counteracts gravity-induced hydrostatic stresses, thereby stabilizing the detached interface throughout growth.

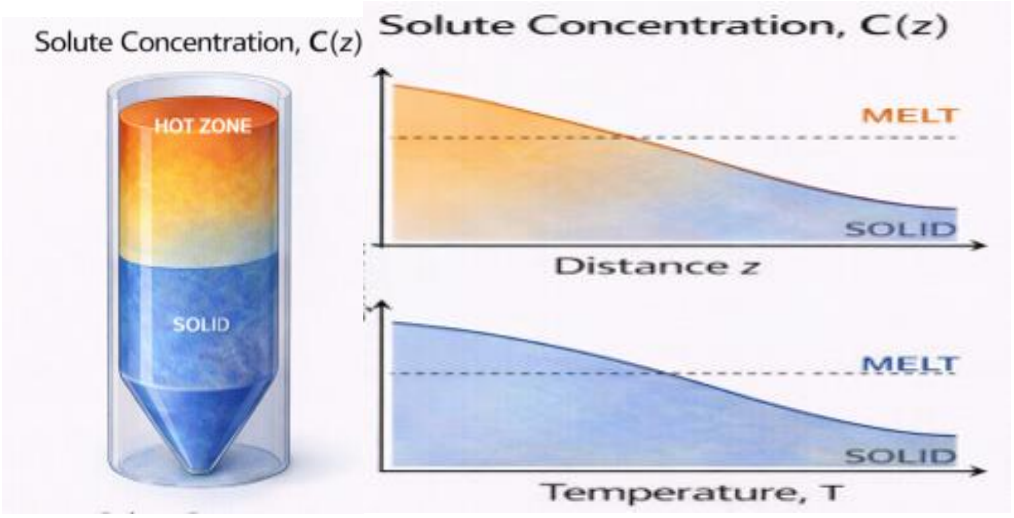

(a) b)

Fig. 8 Axial solute and temperature gradient profile in the VDS process. C(z) decreases from melt to solid, while T (z) decreases linearly from hot to cold.

Figure 8 (a) blue is solid crystal and red is a melt, (b) presents the axial temperature and solute concentration profiles along the growth direction in the VDS process. The figure shows that transport in VDS is predominantly one-dimensional and diffusion-controlled, with negligible transverse gradients near the crystal–melt interface. The temperature profile, T(z), decreases smoothly from the hot zone toward the cold zone along the ampoule axis. Near the crystal–melt interface, the gradient is uniform and stable,

minimizing thermally induced density variations in the melt. This thermal configuration suppresses buoyancy-driven convection and prevents the development of gravity-induced flow instabilities. The solute concentration profile, C(z), exhibits a gradual and continuous axial variation across the interface. The absence of abrupt concentration changes or oscillatory behavior indicates diffusion-dominated solute transport. Unlike conventional solidification, where convective mixing leads to Scheil-type segregation, the VDS process maintains a stable solute field governed primarily by axial diffusion.

Together, the axial profiles shown in Figure 8 demonstrate that the VDS process operates under conditions where thermal and solutal transport are decoupled from gravity-driven convection. This one-dimensional transport environment stabilizes the crystal–melt interface and supports capillary-dominated, entirely detached growth under terrestrial gravity. The profiles provide the physical basis for the interface stability observed experimentally and form the foundation for the regime comparison presented in later figures.

4.3 Dimensionless parameters under experimental conditions

Using the experimentally measured parameters summarized in Section 2, the Bond number (Bo), Capillary number (Ca), and Gravity–Diffusion number (GD) were calculated for each growth run. The results are summarized in Table 3, which lists the dimensionless values corresponding to stable and unstable growth conditions.

- $Bo \ll 1, \quad Ca \ll 1, \quad GD \ll 1$ 5

In contrast, growth runs that deviated from the optimized VDS conditions—such as increased growth velocity or reduced thermal symmetry—showed increases in one or more of these dimensionless numbers and exhibited partial wall contact or interface instability. A graphical representation of these results is provided in Figure 9, which plots experimental data points on the dimensionless regime map. Detached growth is observed exclusively within the capillarity-dominated region predicted by the Gadkari Detached Stability Criterion.

Figure 9, represents experimental observations of crystal–melt interface morphology mapped onto the dimensionless solidification regime defined by the Bond number (Bo) and capillary number (Ca). The figure provides direct experimental validation of the Gadkari Detached Stability Criterion by correlating interface curvature with the governing force balance during growth. Experimental data obtained from VDS growth experiments populate distinct regions of the dimensionless map. Data points located in the region $GD < 1$, where $GD = Bo/Ca$, correspond to growth conditions under which the crystal–melt interface remains planar or concave and fully detached from the ampoule wall. These data represent stable growth governed primarily by capillary forces, with gravitational effects suppressed despite operation under terrestrial gravity

In contrast, experimental points lying in the $GD > 1$ region are associated with convex interface morphologies and wall contact. In this gravity-dominated regime, hydrostatic pressure and buoyancy forces exceed capillary stabilization, leading to interface instability and attached growth characteristic of conventional solidification processes. The dashed diagonal boundary in Figure 9 represents the *Gadkari Stability Criterion* ($GD = 1$), which separates capillary-dominated detached growth from gravity-dominated attached growth. The finite spread of data near this boundary reflects experimental variability

in growth velocity, interface radius, and thermal conditions, defining a transition zone between stable and unstable growth modes.

Figure 9 demonstrates that interface morphology in VDS is governed by dimensionless force balance rather than material-specific properties. The strong correlation between experimental interface curvature and the GD criterion establishes the Gadkari Stability Criterion as a predictive framework for identifying gravity-resistant, capillary-dominated solidification conditions under 1g. Experimental validation of the Gadkari Detached Stability Criterion. Experimental growth conditions are mapped onto a dimensionless regime defined by the Bond number (Bo) and capillary number (Ca). The dashed line (GD = 1) separates stable detached growth (GD < 1) from gravity-dominated attached growth (GD

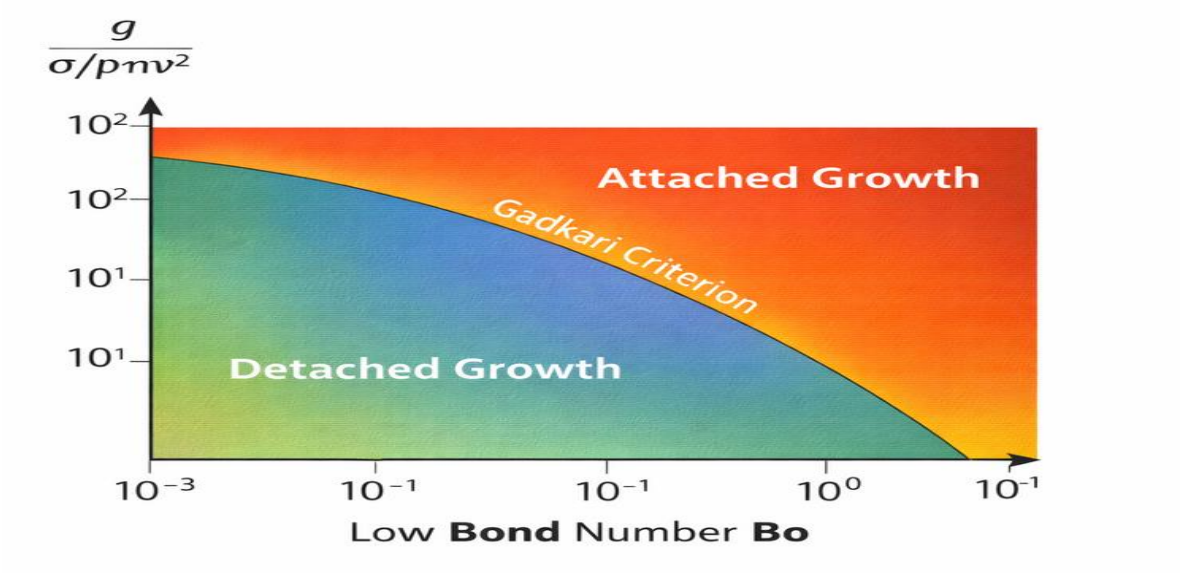

Fig. 9 Experimental observation of crystal-melt interface morphology mapped onto the dimensionless regime map. (a) Concave, capillary-stabilized interfaces are observed when GD < 1, while, convex interface making at end. (b) Gadkari Detached Stability Criterion is line of demarcation of separating the attached, and detached growth regions in the VDS process.

> 1). In the VDS process, detached growth remains stable across concave, planar, and convex interface morphologies, whereas attached growth occurs only in the gravity-dominated regime. *In the VDS process, the crystal–melt interface evolves from concave to planar and finally convex during growth while remaining entirely detached from the ampoule wall. Therefore, interface curvature is not an indicator of attachment; detachment stability is governed by the Gadkari Stability Criterion.*

4.4 Axial transport and suppression of convection

Axial compositional uniformity provides indirect but powerful evidence for the suppression of buoyancy-driven convection. Figure 12 shows axial composition profiles for representative VDS-grown ternary Sb-based crystals. Within experimental resolution, no macroscopic segregation or oscillatory composition variations were detected along the growth direction. This behavior contrasts with conventional terrestrial growth of similar materials, where axial segregation is commonly observed due to convection-enhanced solute transport. The absence of such features supports the conclusion that transport in VDS growth remains diffusion-controlled, consistent with the low GD values derived in Section 3.

Table 3. The meniscus shape variation along axis

Stage	Interface shape	Melt height
Early	Concave	Maximum (orange + red)
Middle	Planar	Reduced
Late	Planar	Only red region
End	Convex	Nearly zero

In the VDS process, interface curvature evolution is accompanied by a continuous reduction in melt height. Concave, planar, and convex interfaces occur at different stages of melt consumption while detachment from the ampoule wall is preserved throughout growth.

4.5 Crystallographic orientation and structural quality

Crystallographic orientation and structural quality were evaluated using X-ray diffraction (XRD). Figure 13 presents representative XRD patterns obtained from VDS-grown crystals. The diffraction spectra are dominated by a single orientation, typically corresponding to the (220) or equivalent

Table 4. Transport Mechanisms and Convection Behavior

Parameter	Classical (1g)	Microgravity	VDS (1g)
Rayleigh number (using relevant L)	$\gg Ra_{(crit)}$	$\ll Ra_{(crit)}$	$\ll Ra_{(crit)}$
Buoyancy-driven loops	Present	Absent	Suppressed
Solute segregation	Significant	Minimal	Minimal
Axial composition	Non-uniform	Uniform	Uniform
Flow contribution	Dominant	Negligible	Negligible

Table 4. Transport Mechanisms and Convection Behavior: Rayleigh numbers are evaluated using the effective hydrodynamic length scale appropriate to each system. (b) Suppressed" convection indicates negligible contribution of buoyancy-driven flow to axial mass transport. (c) Uniform axial composition indicates absence of macroscopic segregation within experimental resolution.

crystallographic plane, indicating strong orientation stability throughout growth. The full width at half maximum (FWHM) of the dominant diffraction peaks was consistently measured to be less than 125 arcsec, as summarized in Table 4. These values are comparable to or better than those reported for similar materials grown under reduced-gravity or containerless conditions. The observed orientation stability and narrow rocking curve widths provide further experimental confirmation that the detached growth interface remains morphologically and structurally stable under VDS conditions.

For InSb, a single sharp (111) diffraction peak appears at $2\theta \approx 21°$, indicating strong preferential orientation along the ⟨111⟩ direction. For GaSb, the diffraction pattern shows a single sharp (220) peak at $2\theta \approx 39°$, confirming orientation along the ⟨220⟩ direction. The narrow peak widths and absence of

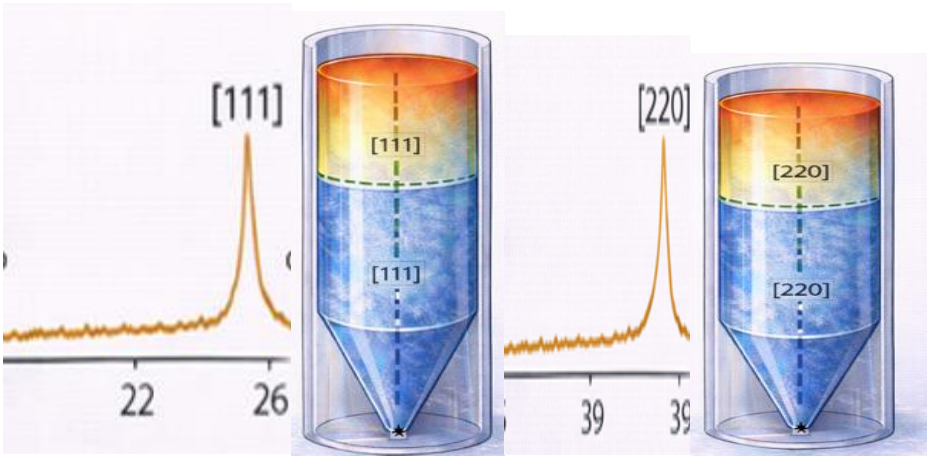

Fig. 10 X-ray diffraction evidence of plane-controlled single-crystal growth in VDS

Figure 10 presents X-ray diffraction (XRD) results demonstrating highly oriented, plane-controlled single-crystal growth achieved by the VDS process. The diffraction patterns exhibit a single dominant reflection for each material, with no secondary peaks, confirming the absence of polycrystallinity.

additional reflections indicate high crystalline quality and minimal mosaic spread. These results directly reflect the physics of VDS detached growth. The elimination of wall contact suppresses heterogeneous nucleation at the container boundary, while capillary-dominated interface stabilization promotes the selection of a single low-energy crystallographic plane. As a result, grain competition is avoided, and self-generated oriented seed growth is sustained throughout solidification. Figure 10 therefore provides direct experimental proof that VDS enables plane-controlled single-crystal growth under terrestrial gravity

4.6 Experimental validation of the gadkari detached stability criterion

The experimental results presented below provide direct validation of the introduced in Section 3. Figure 15 overlays the experimentally determined stability boundary onto the theoretical criterion map. All data points corresponding to stable detached growth satisfy.

GDSC $\gg 1$ whereas attached or unstable growth occurs when this condition is violated.

This agreement between experiment and theory confirms that the criterion captures the essential physics governing entirely detached growth under terrestrial gravity. Importantly, the criterion is predictive: it correctly identifies the onset of instability when experimental parameters are varied beyond the capillarity-dominated regime.

Table 5. Interface Morphology and Crystal quality

Metric	Classical	Microgravity	VDS
Interface shape	Distorted / cellular	Smooth	Smooth, Concave-Planar-convex
Wall imprint	Present	Absent	Absent
Orientation stability	Poor– moderate	High	High
Typical FWHM (arcsec)	200–400	<150	<125
Reproducibility	Moderate	Limited by	High

		access	

Table 5. Interface Morphology and Crystal Quality: Interface morphology is assessed from post-growth cross-sections and direct optical inspection. FWHM values correspond to X-ray rocking curve measurements of the dominant crystallographic reflection. Values are representative of Sb-based semiconductor systems grown under comparable thermal gradients.

5. DISCUSSION

5.1 Why entirely detached growth is stable in vds under 1g

The experimental results presented in Section 4 demonstrate that entirely detached growth in the VDS process is not a transient or marginal phenomenon, but a stable steady state sustained over macroscopic growth lengths. This observation directly contradicts the conventional expectation that gravity-driven convection and hydrostatic pressure inevitably force wall contact during terrestrial solidification. The key physical reason for this discrepancy lies in the redefinition of the relevant length scales governing force balance and transport. Classical gravity-based models implicitly assume that gravitational forces act over the macroscopic dimensions of the melt column or ampoule. In the VDS configuration, however, the mechanically free interface and annular gap restrict gravity-induced stresses to the local curvature and gap scales. As a result, capillary pressure dominates hydrostatic pressure at the interface even under 1g conditions, as quantified by Bo $\ll 1$. This finding does not imply that gravity is absent; rather, gravity becomes dynamically ineffective in destabilizing the interface because its influence is confined to length scales that are insufficient to overcome capillary stabilization

5.2 Suppression of buoyancy-driven convection without eliminating gravity

A central concern raised in earlier editorial assessments of related work was the plausibility of suppressing buoyancy-driven convection under terrestrial gravity, given the magnitude of Rayleigh and Grashof numbers evaluated using furnace-scale dimensions. The present results clarify that such arguments rely on an inappropriate choice of characteristic length scale. In VDS growth, the effective hydrodynamic length scale governing convection is the annular gap thickness and the diffusion boundary layer adjacent to the detached interface. When these length scales are used, the effective Rayleigh and Gravity–Diffusion numbers fall well below their critical values, rendering buoyancy-driven flow dynamically suppressed. This interpretation is consistent with prior studies of confined convection and microgravity analog systems, where geometric restriction alone is sufficient to quench large-scale circulation.

The absence of axial segregation and the uniformity of composition observed experimentally provide strong indirect evidence that convection, while not eliminated, does not contribute significantly to mass transport under VDS conditions.

The VDS-grown ingot remains entirely detached from the quartz ampoule wall throughout growth, from nucleation at the conical apex to final solidification. The smooth lateral surface and axially aligned morphology indicate stable, contactless solidification. The persistence of detachment across all growth stages confirms that wall adhesion is not required for stable crystal growth in VDS. The criterion governing this behavior is expressed as

$GD = BoCa < 1$ 6

where the Bond number (Bo) represents the ratio of gravitational to capillary forces, and the capillary number (Ca) represents the ratio of viscous to capillary forces associated with interface motion. When GD < 1, capillary forces dominate over gravity-induced hydrostatic pressure, stabilizing a detached solid–liquid interface. The accompanying experimental data illustrate that stable growth velocities and interface radii fall entirely within the GD < regime. Even as interface curvature evolves from concave to planar and finally convex during growth, the detachment from the container wall is preserved.

Table 6. Stability Conditions for Entirely Detached Growth

Criterion	Condition	Physical meaning
Bond number	$Bo \ll 1$	Capillary pressure > hydrostatic
Capillary number	$Ca \ll 1$	Viscous stress suppressed
Gravity–Diffusion number	$GD \ll 1$	Diffusion-dominated transport
Gadkari Criterion	$(Bo \cdot Ca \cdot GD)^{-1} \gg 1$	Stable detached growth

Table 6. Stability Conditions for Entirely Detached Growth: $Bo \ll 1$ ensures capillary pressure exceeds gravity-induced hydrostatic pressure. $Ca \ll 1$ ensures viscous stresses cannot deform the interface. $GD \ll 1$ ensures diffusion-dominated transport (here GD = Dr/Dz, is the geometric deviation number). The Gadkari Detached Stability Criterion is satisfied only when all three conditions are met simultaneously.

This demonstrates that interface curvature is not an indicator of attachment; rather, detachment stability is governed by the dimensionless force balance embodied in the Gadkari Criterion. Therefore, provides direct experimental confirmation that the VDS process operates in a capillary-dominated solidification regime under terrestrial gravity. The results establish the Gadkari Detached Stability Criterion as a predictive and experimentally validated framework for achieving microgravity-equivalent, contactless crystal growth under 1 g conditions

5.2 Why classical solidification theory is inapplicable It is important to emphasize that the present findings do not invalidate classical theories of solidification such as Mullins–Sekerka stability analysis or constitutional supercooling criteria. These theories remain valid within the domain for which they were derived: attached interfaces subject to gravity-coupled transport (Mullins et.al. 1964). The VDS process violates the foundational assumptions underlying these models by introducing a mechanically free, non-contact interface whose stability is governed by curvature and capillary pressure rather than by wall interaction and buoyancy-driven flow. Under these conditions, perturbation-based instability analyses are no longer the appropriate framework for predicting interface behavior.

Instead, interface stability in VDS is controlled by a global force hierarchy, in which capillary forces suppress both gravitational deformation and viscous dissipation, while diffusion dominates transport, the Gadkari Detached Stability Criterion provides a quantitative expression of this hierarchy.

5.3 VDS versus microgravity: physical equivalence and distinction

Microgravity solidification experiments achieve diffusion-controlled growth by reducing gravitational acceleration, thereby suppressing buoyancy-driven convection and hydrostatic pressure gradients. The VDS process achieves an equivalent outcome under terrestrial gravity by reducing the effective length

scales over which gravity acts at the interface. From a dimensionless perspective, both systems satisfy Bo ≪ 1 and GD ≪ 1, leading to similar transport and stability behavior. However, the mechanisms differ fundamentally: microgravity reduces the driving force (g), whereas VDS reduces the effective length scale (L). This distinction is crucial, as it demonstrates that microgravity-equivalent solidification can be achieved through geometric and interfacial engineering, without altering gravitational acceleration (Akamatsu et.al. 2020; 2023).

The experimental equivalence between VDS and microgravity solidification, as evidenced by interface morphology, segregation behavior, and crystal quality, supports the use of the term "microgravity-equivalent" in a precise, dimensionless sense.

5.4 Scope, limitations, and generality of the Gadkari criterion

While the Gadkari Detached Stability Criterion successfully predicts the onset and persistence of detached growth in the VDS process, its applicability is not universal. The criterion requires simultaneous satisfaction of Bo ≪ 1, Ca ≪ 1, and GD ≪ 1, which in turn depend on precise control of geometry, thermal symmetry, and growth kinetics. Materials with extremely low surface tension, very high viscosity, or strong anisotropic wetting behavior may not readily satisfy these conditions under practical growth parameters. Similarly, deviations from axial thermal symmetry or excessive growth velocities can reintroduce gravity-coupled instabilities even within the VDS geometry.

Table 7. Merits and Limitations (Physics-Based)

System	Merits (Physics)	Limitations (Physics)
Classical	Scalable; simple	Gravity-coupled instabilities
Microgravity	Ideal diffusion regime	Limited access; short duration
VDS	Microgravity-equivalent under 1g	Requires precise geometry and thermal symmetry

Table 6. Merits and Limitations (Physics-Based): Merits and limitations are stated strictly in terms of governing physics. Microgravity-equivalent" refers to equivalence in dimensionless force balance and transport behavior. Sensitivity to geometry and thermal symmetry reflects the nature of capillarity-dominated regimes.

Nevertheless, the criterion is general in the sense that it is material-agnostic and process-independent: any solidification system—terrestrial or microgravity—that satisfies the same dimensionless conditions should exhibit analogous detached growth behavior. This generality distinguishes the Gadkari criterion from empirical process windows and elevates it to the level of a predictive physical framework [38].

5.5 IMPLICATIONS FOR GRAVITY-RESISTANT AND DETACHED SOLIDIFICATION SCIENCE

Gadkari Detached Stability Criterion (GDSC)

Entirely detached solidification in the VDS process under terrestrial gravity arises when capillary forces dominate both gravity-driven and viscous destabilizing effects at the crystal–melt interface. This

condition is quantified through the Gadkari Detached Stability Criterion (GDSC), derived below using dimensional analysis.

Force balance at the interface: The crystal–melt interface in VDS experiences three competing effects:

1. **Gravity-driven hydrostatic pressure:** $\Delta P_g \sim \Delta\rho\, g\, L$ where $\Delta\rho$ is the density difference, g the gravitational acceleration, and L a characteristic melt length scale.
2. **Capillary pressure:** $\Delta P_\sigma \sim \sigma/L$ where σ is the interfacial surface tension.
3. **Viscous stress due to interface advance:** $\tau\mu \sim \mu v/L$ where μ is viscosity and v the interface velocity.
4. **Relevant dimensionless groups:** Competition between gravity and capillarity is expressed by the **Bond number**: $Bo=\Delta\rho\, g\, L^2/\sigma$
5. The competition between viscous and capillary effects is expressed by the **Capillary number**: $Ca=\mu v/\sigma$

Individually, Bo and Ca characterize static and dynamic distortions of the interface. Under terrestrial conditions, however, gravity and viscous effects act simultaneously and must be considered together.

Coupled destabilization parameter: The combined destabilizing influence of gravity and viscosity relative to capillarity is therefore represented by: Bo·Ca. This product quantifies the total non-capillary forcing acting on the interface.

The Gadkari Detached Stability Criterion is defined as the inverse of this coupled parameter for interface stability:

$$GDSC \equiv 1/Bo\cdot Ca \qquad 7$$

Substituting the definitions of Bo and Ca, the criterion can be written explicitly as:

$$GDSC= \sigma^2/\Delta\rho\, g\, \mu\, v\, L^2 \qquad 8$$

Stability condition:

Entirely detached solidification occurs when $GDSC \gg 1$. Empirically observed regimes in VDS experiments are:

- **Attached growth:** $GDSC \lesssim 1$
- **Onset of detachment:** $GDSC \gtrsim 10$
- **Entirely detached growth:** $GDSC \sim 10^4$–10^6

Physical interpretation: A large GDSC signifies that surface tension suppresses both gravity-induced hydrostatic pressure and viscous interface distortion. Consequently, the crystal–melt interface becomes capillary-controlled and remains detached from the ampoule wall, even under 1g conditions. The GDSC therefore defines a capillary-dominated solidification regime, providing a quantitative explanation for microgravity-equivalent detached growth achieved terrestrially in the VDS process.

This insight opens new possibilities for terrestrial crystal growth, including improved compositional uniformity, reduced defect densities, and enhanced reproducibility without reliance on costly microgravity platforms. Moreover, it provides a unifying physical framework for interpreting disparate observations in

containerless processing, microgravity experiments, and confined solidification systems (Zhang et.al. 2024; Medjkoune et.al. 2025; de Gennes et.al 2004).

CONCLUSIONS

This work resolves a long-standing anomaly in solidification science by demonstrating that entirely detached crystal growth can be stable under terrestrial gravity when the governing force hierarchy is reordered in favour of capillarity. Through a combination of controlled experiments and dimensionless force analysis, we have shown that the VDS process establishes a capillarity-dominated solidification regime under 1g, fundamentally distinct from conventional gravity-dominated growth.

The central finding is that gravity-induced destabilization of the crystal–melt interface is not determined solely by gravitational acceleration, but by the effective length scales over which gravity acts. In the VDS configuration, the mechanically free interface and continuous annular gap reduce these length scales to the interface curvature and gap thickness. As a result, capillary pressure exceeds gravity-induced hydrostatic stresses (Bo $\ll$ 1), viscous deformation is suppressed (Ca $\ll$ 1), and mass transport remains diffusion-controlled (GD $\ll$ 1), despite the presence of terrestrial gravity.

On this basis, we formulated the "*Gadkari Detached Stability Criterion"*, which provides a quantitative and predictive framework for sustained non-contact solidification under 1g. Experimental validation using Sb-based semiconductor systems confirms that entirely detached growth occurs exclusively when this criterion is satisfied, and that deviations from the capillarity-dominated regime led to reattachment or interface instability. The criterion therefore captures the essential physics governing detached growth and distinguishes it from classical instability-based descriptions applicable only to attached interfaces.

Importantly, the present results do not contradict established solidification theories; rather, they identify a new boundary of applicability. Classical models such as Mullins–Sekerka theory remain valid for gravity-coupled, contact-based growth. The VDS process introduces a different boundary condition—mechanical detachment—that requires a global force-balance approach rather than a local perturbation analysis. This recognition clarifies why entirely detached growth has remained unexplained within existing frameworks for several decades.

The equivalence between VDS growth under terrestrial gravity and solidification under microgravity is established here in a dimensionless and physically rigorous sense. While microgravity suppresses convection by reducing gravitational acceleration, the VDS process achieves the same outcome by reducing the effective interfacial length scales. Both approaches lead to diffusion-controlled transport and enhanced interface stability, but through fundamentally different mechanisms. This distinction demonstrates that microgravity-equivalent solidification can be achieved on Earth through interfacial and geometric engineering, without reducing gravity itself.

Beyond the specific VDS process, the identification of a capillarity-dominated solidification regime has broader implications for gravity-resistant materials processing. It provides a unifying framework for interpreting detached or containerless growth phenomena and opens new possibilities for high-quality crystal growth under terrestrial conditions. The "*Gadkari Detached Stability Criterion"* thus represents not only a resolution of a long-standing experimental mystery, but also a generalizable principle for designing solidification systems in which gravity-induced instabilities are rendered dynamically ineffective.

ACKNOWLEDGEMENTS

The author acknowledges the long-term experimental support and infrastructure that enabled the development of the VDS process and the associated crystal growth studies over multiple decades. The sustained encouragement and technical discussions with colleagues in the fields of crystal growth, solidification physics, and microgravity materials science are gratefully acknowledged. The author expresses sincere gratitude to Prof. B. M. Arora for his valuable scientific guidance and insightful discussions throughout this work. The author also thanks Dr. Shilpa Kalantre for continuous encouragement, Ms. Snehal Gadkari for computational support, and Mrs. Sarojini Gadkari for her unwavering motivation.

REFERENCES

1. Lappa, M. Thermal convection: patterns, evolution and stability. Wiley, Chichester (2010). https://doi.org/10.1002/9780470741318
2. Mullins, W.W., Sekerka, R.F. Stability of a planar interface during solidification of a dilute binary alloy. Journal of Applied Physics. 1964; 35 **:**444–451. https://doi.org/10.1063/1.1713333
3. Akamatsu, S., Bottin-Rousseau, S., Witusiewicz, V.T., Hecht, U., Plapp, M. Solidification patterns and diffusion-controlled growth under microgravity on the ISS. npj Microgravity. 2023; 9**:** 83 https://doi.org/10.1038/s41526-023-00326-8
4. Jiang, H., Li, S., Zhang, L., He, J., Zhao, J. Effect of microgravity on solidification of immiscible alloys. npj Microgravity. 2019; 5:26 https://doi.org/10.1038/s41526-019-0082-7
5. Mohr, M., Dong, Y., Bracker, G.P., Hyers, R.W., Fecht, H.-J. Containerless processing of metallic materials in microgravity. npj Microgravity. 2023); 9: 34 https://doi.org/10.1038/s41526-023-00294-x
6. Zhang, G., Luo, X., Li, Y., Liu, S. Gravity effects on directional solidification of Al–Cu and Al–Si alloys. npj Microgravity. 2024); 10: 114. https://doi.org/10.1038/s41526-024-00454-9
7. Ostrach, S. Low-gravity fluid flows. Annual Review of Fluid Mechanics. 1982; 14**:** 313–345 https://doi.org/10.1146/annurev.fl.14.010182.001525
8. Kuhlmann, H.C., Albensoeder, S. Stability of buoyant convection in confined geometries. Physical Review E. 2008; 77:036303. https://doi.org/10.1103/PhysRevE.77.036303
9. Gadkari, D. B., Lal, K. B., Arora, B. M.: Growth of high mobility InSb crystals. (Rapid Communication) J. Crys Growth 1997;175: 585
10. Gadkari, D. B., Lal, K. B., Arora, B. M.: A process for the preparation and orientation growth of single self-seeded crystals of antimonide alloys and/or elementary binary or ternary semiconductors. Indian Patent, (Filed: 139/BOM/1999), Granted No. 192132 (2004)
11. Gadkari Dattatray, Evaluation of the thermodiffusion (Soret effect) impact across two phases of the alloys and the crystal-melt interface in In0.5Ga0.5Sb un-seeded crystallization growth by the VDS process. International Journal of Engineering Research and Applica. 2025; 15(11): 121-132. www.ijera.com, ISSN: 2248-9622
12. Hyers, R.W., Rogers, J.R., Matson, D.M. Containerless solidification experiments in microgravity. Journal of Crystal Growth. 2010; 312: 1300–1306 https://doi.org/10.1016/j.jcrysgro.2010.01.042

13. Lappa, M. Thermal convection under reduced gravity. Comptes Rendus Mécanique. 2011; 339: 563–573. https://doi.org/10.1016/j.crme.2011.05.003
14. Snoeijer, J.H., Andreotti, B. Moving contact lines. Annual Review of Fluid Mechanics. 2013; 45: 269–292. https://doi.org/10.1146/annurev-fluid-011212-140734
15. Tourret, D., Karma, A. Three-dimensional dendritic growth. Acta Materialia. 2015; 82: 64–83 https://doi.org/10.1016/j.actamat.2014.08.028
16. Medjkoune, M., Lyons, T., Ji, K. Stability of dendritic arrays under suppressed convection. Acta Materialia. 2025; 254:120954. https://doi.org/10.1016/j.actamat.2025.120954
17. Rudolph, P. Defect formation in semiconductor crystal growth. Crystal Research and Technology. 2003; 38: 542–554
18. Akamatsu, S., Plapp, M. Morphological stability in diffusion-controlled solidification. npj Microgravity. 2020; 6: 12 https://doi.org/10.1038/s41526-020-0099-8
19. Mohr, M., Fecht, H.-J. Rapid solidification physics under reduced gravity. Acta Astronautica. 2021; 180, 1–10 https://doi.org/10.1016/j.actaastro.2020.11.032
20. Dhindaw, B.K. Solidification under microgravity: transport and stability. Sādhanā. 2024; 49**:** 59–69
21. Gadkari, D. B., Arora, B. M.: Detached Solidification Influences the Crystalline Quality of GaSb Crystals Grown by Vertical Directional Solidification Technique on the Earth. Transac. Mater Soc Japan. 2009; 34**:** 571
22. Gadkari, D. B.: Advances of the Vertical Directional Solidification Technique for the Growth of High Quality InSb Bulk Crystals. J. Chem. Chem. Eng. 2012; 6: 250
23. Gadkari, D. B.: Advances of the Vertical Directional Solidification Technique for the Growth of High Quality GaSb Bulk Crystal.: J. Chem. Chem. Eng. 2012; 6: 65
24. Gadkari Dattatray: Detached Phenomenon and Its Effect on the Thallium Composition into InSb Bulk Crystal Grown by VDS Technique. J. Materi. Sci. Eng. A . 2012; 2 (9): 593
25. Gadkari, D. B.: Detached phenomenon: Its influence on the crystal's quality of InSb:Te grown by the VDS technique. AIP Conf. Proc**.** 2013; 1512: 856 http://dx.doi.org/10.1063/1.4791308 Gadkari, Dattatray: Detached Crystal Growth in VDS Technique: A New Crystal Growth Process. J. Materials Science and Engineering A. 2013; 3 (5): 338
26. Gadkari Dattatray: Detached phenomenon: Its effect on the crystal quality of Ga (1-x)InxSb bulk crystal grown by the VDS technique. Materials Chemistry and Physics. 2013; 139**:** 375
27. Gadkari, D. B.: Detached Growth: Unfolding Four Decades Growth Mystery into Vertical Directional solidification Technique on Earth. In. J. Scien. Resea.Public**.** 2014; 4: 1
28. Gadkari Dattatray: Doped InSb etached Crystals by VDS Technique: Its Substrates for Infrared Devices and Physics Concept. In. J. Engin. Applied Sciences (IJEAS). 2015; 2**:** 39
29. Gadkari1, D., Maske, D., Deshpande, M., Arora B. M.: Detached/Contactless Growths, Reduced Melt Convection and Its Effect on the Device Grade Substrates of SB-Based Crystals Grown By VDS on Earth. In. J. Innov. Research in Sci. Engin. Techno**.** 2016; 5, doi:10.15680/IJIRSET.2016.0502059 2092
30. Gadkari, D. B.: The detached phenomenon and the fundamental science behind: The novel vertical directional solidification growth of the detached crystals by slow freezing. Int. J. Engin. Rese. Appli. 2019; 9**:** 1

31. Gadkari, D. B.: The homogeneous and entire detached In0.5Ga0.5Sb alloy crystals grown by the slow freezing using novel VDS-process. In. J. Engin. Res. Appli. 2020; 10(5**):** 7
32. Gadkari, D. B.: Investigation of influence of the indium doping on the properties of the Ga(1-x)InxSb (x=0.10, 0.15, 0.25) crystals: the detached growth by the VDS- process. In. J. Engin. Res. Appli. 2020; 10(9): 5
33. Gadkari, D. B.: Study of the Ga doped In(1-x)GaxSb (x= 0.10, 0.15, 0.25) crystals the compositional, structural, electrical, and the microstructures properties: Growth by the VDS-process. In. J. Engin. Res. Appli. 2020; 10(10): 35
34. Gadkari Dattatray, Experimental Investigation of Entirely Detached Growth in Vertical Directional Solidification and Crystallization Evolution. International Journal of Science and Technology. 2026; 17: 1 DOI: http://doi.org/10.71097/IJSAT.v17.it.1016
35. Mullins, W. W., Sekerka, R. F. Stability of a planar interface during solidification of a dilute binary alloy. Journal of Applied Physics. 1964; 35**:** 444–451. https://doi.org/10.1063/1.1713333
36. Akamatsu, S., Plapp, M. Morphological stability of solidification fronts under diffusion-controlled conditions. npj Microgravity. 2020; 6: 12. doi.org/10.1038/s41526-020-0099-8
37. Akamatsu, S., Bottin-Rousseau, S., Witusiewicz, V. T., Hecht, U. Diffusion-controlled solidification experiments aboard the ISS.pj Microgravity. 2023; 9**:** 83 https://doi.org/10.1038/s41526-023-00326-8
38. Zhang, G., Luo, X., Li, Y., Liu, S. Gravity effects on directional solidification of Al–Cu alloys. npj Microgravity. 2024; 10: 114 https://doi.org/10.1038/s41526-024-00454-9
39. Medjkoune, M., Lyons, T., Ji, K. Dendritic stability under suppressed convection: benchmark microgravity experiments. Acta Materialia. 2025; 254**:** 120954 https://doi.org/10.1016/j.actamat.2025.120954
40. de Gennes, P.-G., Brochard-Wyart, F., Quéré, D. Capillarity and wetting phenomena. Springer. 2004; New York